EPiC Series in Health Sciences
Volume 8, 2026, Pages 98–102
Proceedings of The 25th Annual Meeting of the International Society for Computer Assisted Orthopaedic Surgery

Statistical Shape Models for the Planning of TKA Surgery

Anna Gounot[134], Marion Decrouez[1], Baptiste Dehaine[1], Guillaume Dardenne[23], and Valérie Burdin[34]

[1] Ganymed Robotics, Paris, France
anna.gounot@ganymedrobotics.com
[2] INSERM, France
[3] LaTIM U1101, Brest, France
[4] IMT Atlantique, Brest, France

Abstract

CT-based methods, such as robotic systems and patient-specific instrumentation (PSI), offer precise bone depiction, making them valuable for Total Knee Arthroplasty (TKA). However, they must be robust to the presence of cartilage, which is not easily visible on CT-scans. We present here a coupled bone and cartilage Statistical Shape Model (SSM) that predicts cartilage solely from bone shape. Four models were trained and tested for healthy and pathological patients, for both femur and tibia. Cartilage prediction results show good adaptability to the pathology as well as similar accuracy compared to the inter-observer MRI manual segmentation variability. This solution could be integrated in the planning of TKA surgeries to improve CT-based PSI and robotic systems.

1 Introduction

Knee osteoarthritis (KOA) affected 365 million people in 2019, with a projected 74.9% increase by 2050 compared to 2020 [8]. Patient-specific instrumentation (PSI) and robotic systems have recently been developed to automate Total Knee Arthroplasty (TKA), to reduce cost, operating time and dissatisfaction rates. Some systems are image-based and require a 3D joint model from preoperative imaging. Studies comparing CT and MR-based PSIs ([13], [16], [7]) draw opposite conclusions, suggesting no clear consensus on the most suitable modality in terms of accuracy. CT-scan is often preferred for its higher availability, shorter scan time and lower cost [13].

However, soft tissues, particularly cartilage, are not easily visible on CT-scan. In CT-based procedures, this absence of cartilage in the preoperative model impacts the accuracy of direct matching with the intraoperative scene, which includes cartilage. One solution is to acquire the bony surface intraoperatively to align with the preoperative bone model, either by exposing bone through cartilage removal [10] or piercing cartilage with a probe to collect bony points [12]. These additional steps may be prone to user error, tedious, and cognitively demanding. An alternative is to preoperatively predict cartilage from bone, enabling direct surface-based registration with the intraoperative scene.

Statistical Shape Models (SSMs) are effective for personalized modeling [9] and for inferring missing shape parts [11]. This study builds on well-established SSM methods for knee cartilage prediction [15] and extends their application to comparing performances on healthy and pathological datasets.

2 Materials and methods

2.1 Dataset

The OAI-ZIB dataset was used, with 507 manual segmentations of femur and tibia bone and cartilage [1]. A normal, narrowed or severe joint space narrowing (JSN) degree was assigned to each patient for both lateral and medial sides. It allowed the grouping of patients into four subdatasets : patients with either premorbid, medial, lateral or bilateral JSN. This study focuses on the premorbid (healthy) and medial (pathological) JSN datasets due to insufficient data in the others for SSM training. They will be referred to as healthy and pathological sets — in terms of JSN — regardless of the presence of osteophytes. The train/test sets distribution was 129/33 and 187/47 for healthy and pathological sets respectively, following a 80/20% ratio.

2.2 Statistical Shape Model

To obtain a coupled SSM that encompasses bone and cartilage, we first trained a bone SSM on the bone mesh of each patient. The bone SSM was then fitted [4] to each patient of the train set to obtain a set of bones in correspondence.

From the corresponding bones, we compute the subchondral vertices as the nearest neighbors of the cartilage mesh on the bone point cloud. We then compute the intersections of the normals of these subchondral vertices with the cartilage surface and obtain a set of cartilage vertices in correspondence, for all the patients in the training set.

A dataset of global bone and cartilage point clouds is computed by merging bones and cartilages in correspondence, on which Principal Component Analysis is applied to obtain a coupled bone and cartilage SSM. The bone part of the coupled SSM can then be fitted to a new patient whose cartilage is unknown to predict the missing cartilage.

Four coupled SSMs were generated, for healthy and pathological femurs and tibias.

2.3 Evaluation metrics

The coupled bone and cartilage SSM was validated using standard metrics from [14]. The cartilage thickness among the training set was computed as the distance between subchondral bone and cartilage intersection points along the normal, based on the cartilage correspondences' establishment method (2.2). The cartilage prediction among the testing set was assessed as the point-to-surface distance between the predicted cartilage point cloud and the patient bone and cartilage mesh.

3 Results

Maps of mean cartilage thickness are presented in figure 1. Mean cartilage thickness was 1.9 mm (95th percentile: 4.2 mm) for healthy femurs, 1.9 mm (4.3 mm) for pathological femurs, 1.1 mm (3.7 mm) for healthy tibias, and 1.1 mm (3.8 mm) for pathological tibias. The 95th percentile provided a robust estimate of maximum thickness, minimizing outlier influence. Cartilage prediction results are presented in figure 2. Prediction RMSE was 0.8 mm for pathological femur and 0.7 mm for all other three cases.

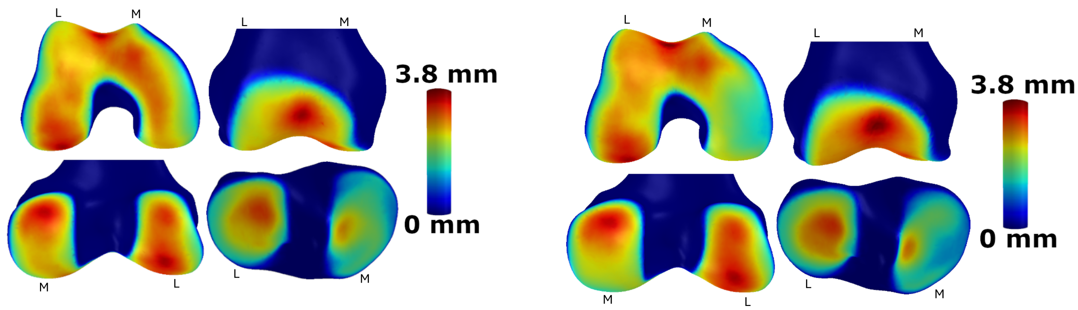

(a) Healthy (b) Medial pathology

Figure 1: Maps of mean cartilage thickness, for healthy and pathological patients of the train set. Lateral and medial sides are indicated by the letters L and M.

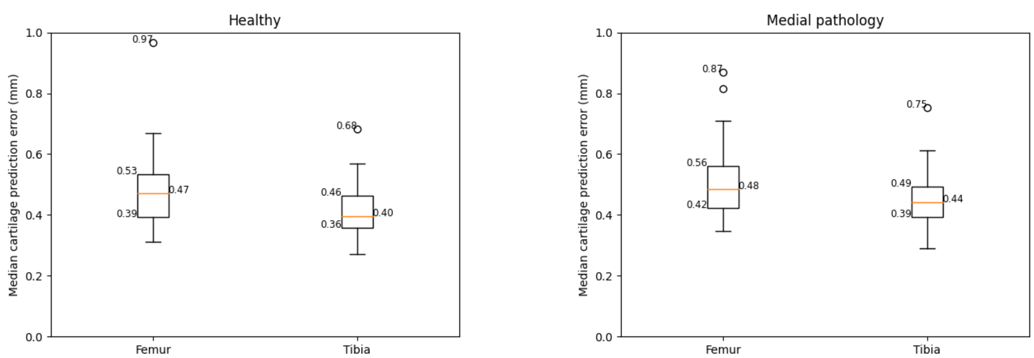

(a) Median error boxplot - Healthy (b) Median error boxplot - Medial pathology

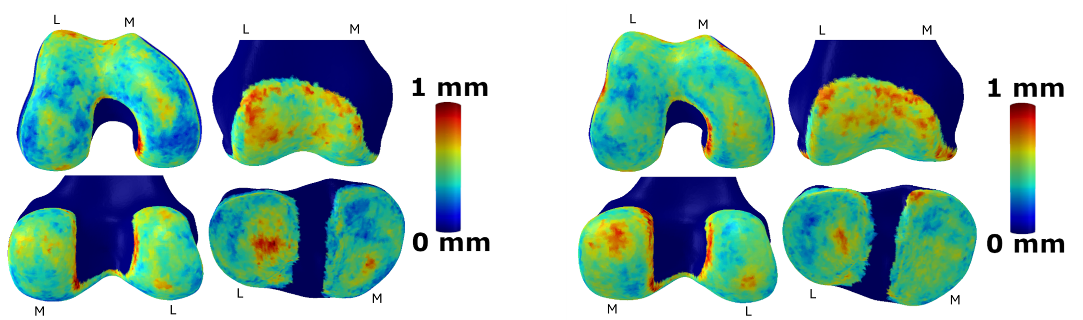

(c) Median error map - Healthy (d) Median error map - Medial pathology

Figure 2: Cartilage prediction median errors for the healthy (left) and pathological (right) test sets. (a), (b) For each patient, the median error across all cartilage vertices was computed. Boxplots summarize the distribution of these patient-wise median errors. (c), (d) For each vertex, the median error across all patients was computed to generate error maps. Lateral and medial sides are indicated by the letter L and M.

4 Discussion

We presented a method for predicting cartilage surface from bone shape, for healthy and arthritic knees.

Cartilage thicknesses are consistent with the literature [2] and show expected medial loss in medial KOA. Similar mean and 95th percentile thicknesses across groups indicate that pathology causes cartilage thinning in specific areas, with comparable thickness elsewhere in the joint.

Cartilage prediction errors remain well below the maximal observed 95th percentile thickness of 4.3 mm. RMSE around 0.7 mm is close to [15], with slightly higher values likely due to a smaller training set. It is also similar to inter-observer variability in manual MRI segmentation [6], suggesting that SSM-based cartilage prediction from a CT-scan is an interesting alternative to MRI cartilage segmentation. Errors along the cartilage surface outline (figure 2) may result from osteophytes which are highly patient-specific and can lead to poorly established correspondences in these regions. Additionally, osteophyte formation is non-linear and may not be well captured by SSMs [5]. Still, similar prediction errors in healthy and pathological patients suggest that our model effectively models KOA and its impact on cartilage. This study demonstrates the applicability of SSMs to pathological cases.

However, limitations remain. The models were trained and tested on different numbers of patients, affecting comparability. A larger dataset is needed for better evaluation. Additionally, cartilage was predicted from bone MRI segmentations rather than CT-scans, ignoring potential MRI-CT bias [3].

References

[1] Felix Ambellan, Alexander Tack, Moritz Ehlke, and Stefan Zachow. Automated segmentation of knee bone and cartilage combining statistical shape knowledge and convolutional neural networks: Data from the osteoarthritis initiative. *Medical Image Analysis*, 52:109–118, February 2019.

[2] G.A. Ateshian, L.J. Soslowsky, and V.C. Mow. Quantitation of articular surface topography and cartilage thickness in knee joints using stereophotogrammetry. *Journal of Biomechanics*, 24(8):761–776, 1991.

[3] Alan Brett, Michael A. Bowes, and Philip G. Conaghan. Comparison of 3d quantitative osteoarthritis imaging biomarkers from paired ct and mr images: data from the imi-approach study. *BMC Musculoskeletal Disorders*, 24(1), January 2023.

[4] Tim Cootes, ER Baldock, and J Graham. An introduction to active shape models. *Image processing and analysis*, 328:223–248, 2000.

[5] Anthony A. Gatti, Louis Blankemeier, Dave Van Veen, Brian Hargreaves, Scott L. Delp, Garry E. Gold, Feliks Kogan, and Akshay S. Chaudhari. Shapemed-knee: A dataset and neural shape model benchmark for modeling 3d femurs. *IEEE Transactions on Medical Imaging*, 44(3):1140–1152, March 2025.

[6] Tobias Heimann, Bryan Morrison, Martin Styner, Marc Niethammer, and Simon Warfield. Segmentation of knee images: A grand challenge. *Proc. MICCAI Workshop on Medical Image Analysis for the Clinic*, 01 2010.

[7] Dong-Geun Kang, Kang-Il Kim, and Jung-Kwon Bae. MRI-based or CT-based patient-specific instrumentation in total knee arthroplasty: How do the two systems compare? *Arthroplasty*, 2(1):1, January 2020.

[8] Huibin Long, Qiang Liu, Heyong Yin, Kai Wang, Naicheng Diao, Yuqing Zhang, Jianhao Lin, and Ai Guo. Prevalence trends of site-specific osteoarthritis from 1990 to 2019: Findings from the global burden of disease study 2019. *Arthritis & Rheumatology*, 74(7):1172–1183, June 2022.

[9] David Lüdke, Tamaz Amiranashvili, Felix Ambellan, Ivan Ezhov, Bjoern H. Menze, and Stefan Zachow. *Landmark-Free Statistical Shape Modeling Via Neural Flow Deformations*, page 453–463. Springer Nature Switzerland, 2022.

[10] Lorenzo Mattei, Pietro Pellegrino, Michel Calò, Alessandro Bistolfi, and Filippo Castoldi. Patient specific instrumentation in total knee arthroplasty: a state of the art. *Ann. Transl. Med.*, 4(7):126, April 2016.

[11] Asma Salhi, Valerie Burdin, Arnaud Boutillon, Sylvain Brochard, Tinashe Mutsvangwa, and Bhushan Borotikar. Statistical shape modeling approach to predict missing scapular bone. *Annals of Biomedical Engineering*, 48(1):367–379, September 2019.

[12] Veenesh Selvaratnam, Andrew D. Toms, and Vipul I. Mandalia. Robotic assisted patellofemoral joint replacement: Surgical technique, tips and tricks. *Indian Journal of Orthopaedics*, 56(12):2110–2118, October 2022.

[13] Paul Stirling. Computerised tomographyvsmagnetic resonance imaging for modeling of patient-specific instrumentation in total knee arthroplasty. *World Journal of Orthopedics*, 6(2):290, 2015.

[14] Martin A. Styner, Kumar T. Rajamani, Lutz-Peter Nolte, Gabriel Zsemlye, Gábor Székely, Christopher J. Taylor, and Rhodri H. Davies. *Evaluation of 3D Correspondence Methods for Model Building*, page 63–75. Springer Berlin Heidelberg, 2003.

[15] Christophe Van Dijck, Roel Wirix-Speetjens, Ilse Jonkers, and Jos Vander Sloten. Statistical shape model-based prediction of tibiofemoral cartilage. *Computer Methods in Biomechanics and Biomedical Engineering*, 21(9):568–578, July 2018.

[16] Xiang-Dong Wu, Bing-Yan Xiang, Martijn G.M. Schotanus, Zun-Han Liu, Yu Chen, and Wei Huang. Ct- versus mri-based patient-specific instrumentation for total knee arthroplasty: A systematic review and meta-analysis. *The Surgeon*, 15(6):336–348, 2017.